

Synopsis

Fast electron- and ion-collisions with diatomic and large bio-molecules

Madhusree Roy Chowdhury

Guide : Dr. Chetan G Limbachiya

Department of Applied Physics

Faculty of Technology and Engineering

The Maharaja Sayajirao University of Baroda

Co-guide : Prof. Lokesh C Tribedi

Department of Nuclear and Atomic Physics

Tata Institute of Fundamental Research

October 2020

This thesis describes different aspects of fast electron and ion collisions with atoms, small molecules and large biomolecules. The Young type interference effect in multi electronic diatomic molecules, N_2 and O_2 under fast electron impact were investigated from the present experiments. In addition, detailed measurements of double differential, single differential and total ionization cross sections for e-impact on N_2 are studied over an energy range of 3 -to- 8 keV. We have further investigated the ion impact ionization of uracil, a nucleobase of RNA and bromouracil. The double differential cross section for electron emission from uracil and bromouracil were measured in case of keV energy proton impact. This study was further extended for MeV energy highly charged ions like C^{6+} ions. Apart from obtaining the absolute double differential cross sections (DDCS), we have further investigated the amount of enhancement in electron emission from bromouracil compared to that for uracil. All the e-DDCS measurements were compared with different state-of-the-art theoretical models like the CB1, CTMC and CDW-EIS. In addition, the CSP-ic model was used to obtain the total ionization cross section in case of electron impact. The present study is divided into the following eight chapters.

Chapter 1 : Introduction

The interaction of a charged particle with an atom or molecule provides crucial information about the interacting particles at a microscopic level. When an energetic charged particle collides with an atom or molecule, one of the inelastic processes between the projectile and the target is the Coulomb ionization process, where free electrons are emitted from the target species. The charge state of the projectile q_p , it's velocity v_p , and their ratio i.e, q_p/v_p or the perturbation strength are governing factors to ascertain which process will have predominance over the others [1]. In case of simple target systems like H, He, H_2 , there is an overall and reasonable understanding of the reaction dynamics. But, as the electron number increases in the target system, the complexity increases further and particularly for theoretical models several approximations come into picture. In such cases, accurate experimental measurements are required to test the efficacy of the different theoretical models. Typically, using the traditional electron spectroscopy technique one measures the double differential cross section (DDCS) of the electrons emitted from the target. The energy of the ejected electrons are measured along with their angle of emission. The DDCS measurements provide a much detailed understanding of the collision mechanism than the total cross sections. In the present thesis work we have measured the absolute DDCS of electron emission from different targets when bombarded by fast electrons, keV energy protons and MeV energy C^{6+} ions. The range of targets studied here varied from atoms like helium to small molecules like N_2 , O_2 and CH_4 and further to large biomolecules, uracil and bromouracil. From the measured DDCS, the single differential cross section (SDCS) were obtained by performing numerical integration over the emitted energy or angle and upon further integration, the total ionization cross section (TCS) was derived for each collision system.

Apart from studying the collision dynamics of different projectile-target systems, these measurements have wide scale applications both fundamentally as well as for different other fields of reserach. Two different aspects have been investigated in details in the present thesis work. The diatomic molecules O_2 and N_2 were used for studying the Young type interference effect under the impact of fast electrons. The two atoms in such a diatomic molecule are now known to resemble the two slits of

Young's double slit experiment [2, 3, 4, 5]. Such an interference effect in case of H₂ molecules have already been shown by different groups [3, 6]. However for N₂ and O₂ targets, such an effect has been debated. In case of photoionization, the interference oscillations are clearly observed [7] whereas for heavy ion impact it is non-conclusive [8, 9]. Therefore it would be of interest to understand this phenomenon in case of fast electron impact ionization of N₂ and O₂ molecules.

Ionization studies of biomolecules and water have emerged as a new field of research over the past decade and extensive studies are being carried out both experimentally and theoretically due to its application in cancer treatment [10, 11]. Hadron therapy is one of the promising technique for treatment of malignant tissues. If the tumour is deep inside the human body, then ions are preferential over photons or electrons, particularly for having favourable dose-depth distribution. The ion deposits maximum energy at the end of the track and hence maximum interaction takes place with the biological cells in this region known as the Bragg peak [12]. Extensive measurements have been performed with protons and bare C ions at different energy regimes to understand the ionization behaviour of two biologically relevant molecules, uracil and its halogenated derivative bromouracil.

Chapter 2 : Experimental Techniques

All the experiments for the present thesis work have been carried out using the electron spectroscopy technique. Complimentary modifications to the pre-existing electron spectroscopy set up were done to satisfy the needs of the present experiments. The set up consists of a high vacuum stainless steel scattering chamber which was maintained at a base vacuum of $\sim 5 \times 10^{-8}$ mbar using a turbo molecular pump backed by a tri-scroll pump. The hemispherical electrostatic energy analyzer was placed on a motorized turntable inside the main scattering chamber. The analyzer is capable of measuring the energy and angular distributions of the electrons emitted from the target atom/molecule upon ionization by different projectiles. The projectile beam was collected on a Faraday Cup which was kept electrically isolated from the scattering chamber. Between the main scattering chamber and the beam line, a differential pumping arrangement was used for all the experiments. The experiments were performed under both static gas pressure condition as well as by using an effusive jet source. The gaseous targets were injected inside the scattering chamber using a solenoid valve. In case of static pressure, the entire scattering chamber was flooded with the target gas at a suitable pressure to maintain single collision condition. A capacitance manometer (MKS Baratron) was used to measure the absolute pressure of the target gas inside the chamber. Some of the complementary gas target experiments were also performed using a stainless steel effusive jet source. In case of the experiments with uracil and bromouracil, an effusive vapour jet source was prepared which was made of copper. The powders were heated in a metallic oven which was further mounted inside a water cooled jacket. A thickness monitor was placed above the jet nozzle to account for steady flow of the vapour jet. All these were together made as a single target holder assembly, attached to a 3D translation stage manipulator for proper alignment of the jet nozzle. The target holder assembly was fabricated for this thesis work.

Hemispherical electron energy analyzer

The two hemispheres of the analyzer was made of oxygen free high conductivity (OFHC) copper having an inner and outer radii of 25 mm and 35 mm respectively. The voltages were applied at the two electrodes in such a manner that the electrons of a particular energy passed through the middle of the two hemispheres following an equipotential path [13]. The energy analyzed electrons traveling through the hemispheres were finally detected by a CEM placed after the exit slit of the spectrometer. The resolution of the analyzer was $\sim 6\%$ of the electron energy [14].

Beamline for electron gun

The electrons of keV energy were obtained from a commercially available electron gun. The beamline comprising of sets of Einzel lenses, electrostatic deflectors and several apertures of different diameters were used to focus and collimate the projectile electrons. A pair of magnetic coils were further introduced in the beamline which helped in steering the beam. The use of the magnetic coils resulted in an excellent beam transmission through the spectrometer, ensuring a well collimated parallel electron beam. Several tests were performed to ensure that there was no field effect near the interaction region due to the voltages applied on the deflectors and other electrodes. The electron beam of different energies varying from 3 keV to 8 keV were used for the present series of measurements.

ECR Ion Accelerator

The ECRIA is used for generating low energy highly charged ions. The positively charged ions are produced inside the plasma source which is confined within strong magnetic field. The ions are extracted by applying an extraction field of 30 kV and a 90° bending dipole magnet is used to select the desired ions. The plasma chamber, Einzel lens and the bending magnet are all placed together on an isolated high voltage deck which can be raised upto 400 kV. The analyzing magnet is followed by an accelerating column. Electrostatic triplet quadrupole lenses and electrostatic X-Y deflectors are used to focus the energy and charge state analyzed projectile beam. Beyond this point lies the switching magnet which helps to steer the beam in the desired beamline. The ECRIA has four different beamlines. The electron spectroscopy assembly is connected to the 50° N beamline. The beamline is equipped with electrostatic triplet quadrupole lenses, several deflectors, Faraday Cup and two sets of four-jaw slits for cutting the beam. At the entrance of the experimental set-up there are apertures for further beam collimation. Several sets of turbo molecular pumps and rotary pumps are used to maintain high vacuum of the order of 10^{-9} mbar in the accelerating column and all the beamlines.

Chapter 3 : Theoretical Models

The DDCS measurements for all the various collision systems studied in the present thesis were compared with different state-of-the-art theoretical models which were obtained from our collaborators.

The DDCS for ionization of N_2 under the impact of keV energy electrons were compared with the CB1 and CTMC model calculations. The CB1 model is developed within the framework of the 1st Born approximation with correct boundary

conditions. Here, the partial-wave expansion formalism is used for describing the electron- induced ionization of multielectronic targets [15]. The incident/scattered electron is described by a plane wave whereas the ejected electron is modelled by a Coulomb wave. The classical trajectory Monte Carlo (CTMC) method is a non-perturbative method, where classical equations of motions are solved numerically [16]. In CTMC approach, the many-body interactions are exactly taken into account during the collisions on a classical level. The interaction between the active target electron and the projectile is Columbic in nature.

The DDCS measurements involving keV and MeV energy ion impact ionization of different target molecules (He, CH₄, O₂, uracil and bromouracil) were compared with the CDW-EIS model calculations. The continuum distorted wave-eikonal initial state (CDW-EIS) model is effective both for the intermediate and high velocity regime of the projectile [17]. This is the main advantage of this model over majority of the other fundamental atomic collision models which are perturbative in nature and hence are effective when the velocity of the projectile is sufficiently high.

In addition to the different models mentioned above which were employed to check with the DDCS measurements, the total ionization cross section (TCS) for electron impact on N₂ were compared with the CSP-ic model. The complex scattering potential-ionization contribution (CSP-ic) model, a semi-empirical model is used to calculate the TCS for electron impact on any target atoms/molecules. In this model the projectile electron energies vary from threshold to few keV [18].

Chapter 4 : Young type interference oscillations

Electron emission from a homonuclear diatomic molecule can give rise to one of the important quantum mechanical aspect, the Young type electron interference effect. In case of homonuclear diatomic molecules like H₂, N₂ or O₂, the two atoms are indistinguishable and the electrons can be emitted coherently such that the electron waves are in phase or out of phase. In case of a particle scattering from two identical centres, using the prescription of Messiah [19], the DDCS for electron emission (e.g., for N₂) following dipole approximation may be expressed as

$$\frac{d^2\sigma_{N_2}}{d\epsilon d\Omega} = \frac{d^2\sigma_{2N}}{d\epsilon d\Omega} \left[1 + \frac{\sin(kc(\theta)d)}{kc(\theta)d} \right] \quad (1)$$

where $\frac{d^2\sigma_{2N}}{d\epsilon d\Omega}$ represents the DDCS from the individual nitrogen atoms and k is the outgoing electron momentum in a.u. The term within square brackets represent the interference caused by the two N atoms and is referred here as the Cohen-Fano term [2]. Here d is the internuclear distance and $c(\theta)$ is the adjustable frequency parameter, as introduced by Tribedi and coworkers [4]. The above expression was derived by taking an average over all possible orientations of the molecular axis with respect to the beam direction. There are two different ways of extracting the information contributing from the interference effect.

DDCS Ratios

From eq. 1 it may be noticed that if the DDCS for N₂ is divided by twice the DDCS for atomic N (obtained from theory), then what remains is the contribution from the interference effect. Clear signatures of oscillations were observed from the DDCS ratios as a function of electron velocity. Such ratios were derived for all the different

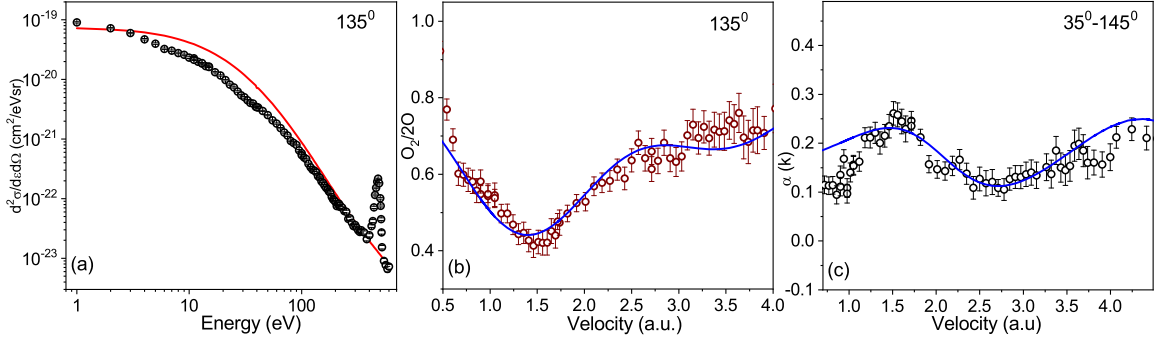


Figure 1: (a) Absolute electron DDCS for 7 keV e^- impact on O_2 , solid line showing theoretical DDCS for twice of atomic oxygen (b) DDCS ratio (σ_{O_2}/σ_{2O}) (c) Asymmetry parameter ($\alpha(k)$) for 30° and 145° .

emission angles and in each and every case the oscillations were observed. The ratios were fitted with the interference term in eq. (1). The frequency parameter $c(\theta)$ being a function of emission angles, the variation of the frequency of oscillation over emission angles were obtained. Similar exercise was also performed for O_2 target and here also the interference oscillations were revealed clearly. Fig. 1 shows one such representative plot for 7 keV e^- impact on O_2 . In Fig. 1(a), the experimental DDCS for O_2 and theoretical DDCS for $2O$ at 135° are plotted and the ratio between the two are shown in Fig. 1(b). The experimental-to-theoretical DDCS ratio shows a nice half sinusoidal oscillation and the blue solid line corresponds to the fitting using the interference term from eq. 1. It is observed that the fitting shows an excellent agreement with the DDCS ratio for a definite value of the the frequency parameter $c(\theta)$.

Forward-backward angular asymmetry

The asymmetry existing in the forward and backward angles is another tool to check for the oscillations. It was first shown by Tribedi et al that forward backward angular asymmetry can be conveniently used to explore the interference oscillation [4]. The forward-backward asymmetry is caused due to the two-center effect and the non-Coulombic nature of the target potential for a multielectronic atom or molecule. In case of electron impact ionization, two center effect doesn't play a major role and hence non-Coulombic potential for the multi-electronic molecule gives rise to the angular asymmetry between forward and backward angles. This can be quantitatively obtained from the difference in the DDCS for small forward and large backward angles. The asymmetry parameter $\alpha(k)$ is defined as [20]

$$\alpha(k, \theta) = \frac{\sigma(k, \theta) - \sigma(k, \pi - \theta)}{\sigma(k, \theta) + \sigma(k, \pi - \theta)} \quad (2)$$

where the electron energy $\epsilon_k = \frac{k^2}{2}$ in a.u. and θ is a low forward angle. The asymmetry parameter does not take into account any consideration of the atomic cross sections. $\alpha(k)$ is obtained only from the measured molecular DDCS for forward and backward angles. In case of O_2 molecule, $\alpha(k)$ again showed clear evidence of interference oscillation implying coherent electron emission from the target molecule. Fig. 1(c) shows the asymmetry parameter as a function of ejected electron velocity for O_2 when performed for 35° and 145° . A complete sinusoidal oscillation is observed

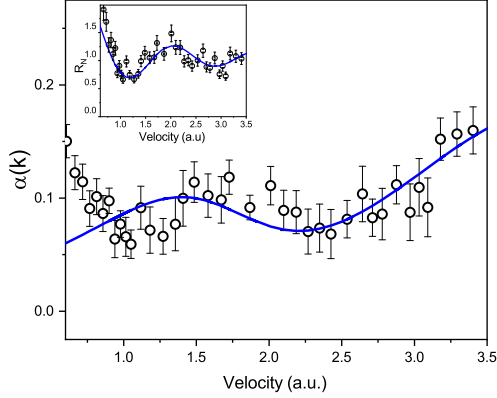


Figure 2: Asymmetry parameter ($\alpha(k)$) for 7 keV e- impact on N_2 . Solid line shows the model fitting, Inset : asymmetry parameter divided by 1st order fitting function.

for the electron velocity between 0.7 and 4.45 a.u. Replacing the DDCS for the two complementary angles in eq. 2 by the DDCS of diatomic molecule given in eq. 1, one obtains an expression of the asymmetry parameter $\alpha(k)$ which contains the sinusoidal term with $c(\theta)$ along with a free parameter β which is the ratio of the frequency between the two complementary angles. The solid line in Fig. 1(c) shows the fitting of the asymmetry parameter for $\beta=1.14$ and is seen to match well with the experimental data points. Overall asymmetry parameter, devoid of any theoretical calculations and normalization factors, provide an excellent method for revealing the interference oscillations.

Second order Interference effect

In addition to first order scattering, there can also be contributions from higher order scattering mechanism [21, 6]. In Fig. 2 we have shown the asymmetry parameter obtained for 7 keV e^- impact on N_2 . A nice oscillatory structure is observed around 0.1. When the $\alpha(k)$ values are fitted for a particular β , it is observed from Fig. 2 that although the fitted curve (blue solid line) matches well beyond 1.5 a.u., but in the low electron velocity region, a periodic deviation exists. Such a deviation indicates the presence of second order scattering effects which will generate a higher frequency component in oscillation. This effect occurs when a particle after getting scattered from one center moves towards the second center and finally gets scattered off the second center. Thus an additional path length is introduced generating higher oscillation frequency. The $\alpha(k)$ values in Fig. 2 are divided by the first order model fitting which further reveal an oscillatory structure (inset of Fig. 2) and when fitted by the Cohen-Fano type fitting produces an oscillation frequency almost double that of primary oscillation. This indicates the signature of second order scattering mechanism for N_2 , however no such effect was observed for O_2 .

Chapter 5 : Electron impact ionization of N₂ : Energy dependence of e-DDCS, SDCS and TCS

Absolute DDCSs measurements were performed for single ionization of N₂ molecule under the impact of fast electrons having energies from 3 to 8 keV at an interval of 1 keV. For each beam energy, the electrons emitted from N₂ were scanned in the energy range from 1 to 500 eV for different emission angles between 30° and 145°. For each angle the spectrum was collected both in the presence and absence of target gas which was further used to eliminate any kind of systematic error. The DDCS decreases rapidly with increase in the ejected electron emission energy. The experimental measurements were also compared with two different theoretical models, i.e., the CB1 and the CTMC models. The CTMC model was calculated for atomic nitrogen which was further multiplied by a factor of 2 to compare with the data. The CTMC model provided very good agreement with the data. On the other hand, the CB1 model showed a qualitative agreement but quantitatively underestimated the data. The K-LL Auger peak corresponding to inner shell ionization from nitrogen was seen distinctly for all the spectra. The angular distributions revealed all the different features of collision processes depending on the energy of the ejected electrons. The binary encounter mechanism was revealed nicely from the angular distributions both by the experimental measurements as well as by the theoretical calculations. The measured DDCSs were integrated further over the emission energies or emission angles to obtain the single differential cross sections (SDCS). They were also compared with the theoretical models. The SDCS were further integrated to generate the total ionization cross section (TCS) for each of the collision systems. As ionization studies were performed for different projectile energies, the dependence of the TCS as a function of beam energies were generated. The TCS were compared with both the above mentioned model calculations as well as with the CSP-ic model. The experimental measurements along with the three model calculations showed overall good agreement qualitatively although some deviations existed quantitatively.

Chapter 6 : Ion impact ionization of atoms and molecules: Comparative study at keV and MeV energy

To study the aspects of ion impact ionization, several experimental measurements were performed for keV energy proton impact on helium, and molecular targets like methane and oxygen. 200 keV protons obtained from the ECRIA were collided with the target atom/molecules in the scattering chamber. In contrast to keV energy protons, collision studies were also performed for MeV energy C⁶⁺ ions interacting with O₂ molecules. 5.5 MeV/u bare C ions were generated from the BARC-TIFR Pelletron accelerator at TIFR. The perturbation strengths (q_p/v_p) for 200 keV protons and 5.5 MeV/u C⁶⁺ ions are 0.35 and 0.40 respectively. These two projectiles were chosen such that although their individual charge state (q_p) and velocity (v_p) are widely different, but, their perturbation strength (q_p/v_p) is nearly the same. For each and every case, the measured cross sections were compared with the CDW-EIS predictions.

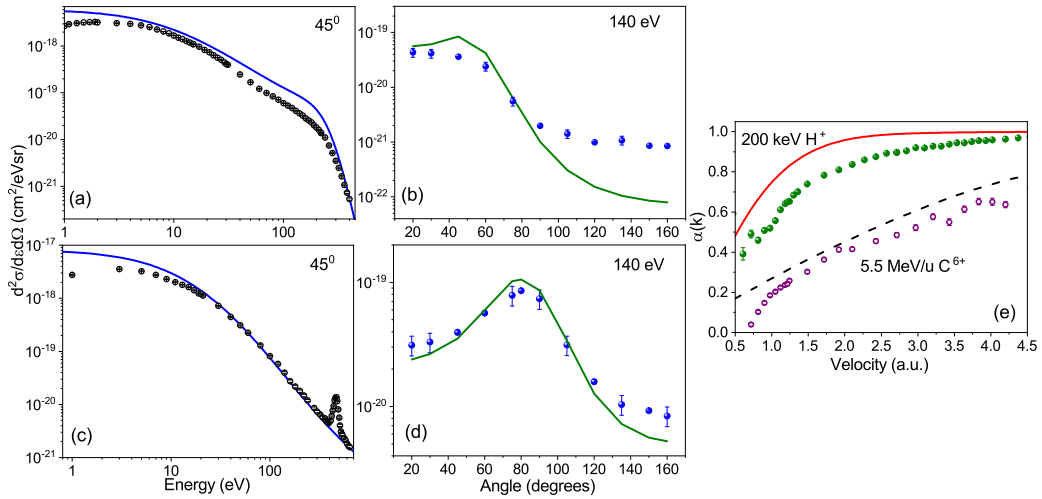


Figure 3: Upper panel show 200 keV proton impact on CH_4 (a) energy distribution (b) angular distribution; Lower panel for 66 MeV C^{6+} ion impact on O_2 (c) energy distribution (d) angular distribution. (e) $\alpha(k)$ for 200 keV proton and 66 MeV C^{6+} ion impact on O_2 as a function of electron emission velocity. Solid and dashed lines in all the panels correspond to the CDW-EIS calculations.

Energy distribution

The cross section fall by few orders of magnitude in the measured energy range of hundreds of eV. Fig. 3(a) show the energy distribution plot for 200 keV proton impact on CH_4 at emission angle 45° . In case of forward angles the binary encounter peak smears over the spectrum, producing a hump like structure around 200 eV (Fig. 3(a)) for 45° and hence the K-LL Auger lines are not visible. The data for 5.5 MeV/u bare C ions colliding with O_2 were collected between 1 and 600 eV for 12 different emission angles. In this case the velocity of the projectile being quite high, the binary peak is present at very high emission energy. Fig. 2(c) display the energy distribution for 5.5 MeV/u C^{6+} ion impact on O_2 . The K-LL Auger peak for oxygen (~ 480 eV) are seen at all the forward and backward angles. In the plots, the low energy region is contributed by the soft collision mechanism. The intermediate part of the spectrum is dominated by the two-center effect, where the emitted electron is under the influence of both the projectile and the receding recoil ion. The experimental data were compared with the CDW-EIS calculations. The agreement is seen to be best for 5.5 MeV/u bare C ions impacting on O_2 (Fig. 3(c)) whereas some deviations existed for 200 keV proton impact data. For He, the theory overestimated the data in the low energy regime and underestimated the data beyond 100 eV for backward angles. Relatively better agreement was observed for 200 keV proton impact on CH_4 . The theoretical predictions had maximum discrepancy in case of proton impact on O_2 molecules.

Angular distribution

The angular distribution of emitted electrons from He, CH_4 and O_2 under the impact of 200 keV protons have distinctly different characteristics to that observed for 66 MeV bare C ions. One such representative plot for 200 keV proton impact on CH_4 (Fig. 3(b)) and 5.5 MeV/u C^{6+} impact on O_2 (Fig. 3(d)) are shown. In case of keV energy proton impact, the cross section is seen to be largest for the extreme

forward angles and goes down gradually with increase in emission angles. The angular asymmetry varies by order of magnitude even for low emission energies and this asymmetry increases further for higher electron energies. The CDW-EIS model predicts similar kind of behaviour qualitatively although quantitatively it underestimates the data in the backward angles. Such large angular asymmetry occur due to the dominance of post collision interaction with the projectile and two-center effect. In case of MeV energy C^{6+} ion impact on O_2 , the angular distribution doesn't show such high asymmetry. For the lowest electron energies (not shown here), the DDCS remain almost flat over the entire angular spread revealing the dominance of soft collision mechanism. For higher emission energies, the DDCS for forward angles are relatively higher compared to the backward angles and a peak like structure appears around 80° corresponding to the binary nature of collision (as seen in Fig. 3(d)) [22]. Although in the present case angular asymmetry exists between the forward and backward angles since the emitted electrons experience a forward attraction along the direction of the highly charged ion, but is not as large as that observed for 200 keV proton impact. The CDW-EIS model calculations which is known to take into account the effect of post collision interaction and two center effect, matches very well with the data points except at the large backward angles.

Asymmetry parameter

The angular asymmetry parameter $\alpha(k)$ defined by eq. 2 is used to obtain the difference in DDCS between low forward angle and its complementary backward angle and thus provides a quantitative estimate of the angular asymmetry. As already seen from Fig. 3, due to the large angular asymmetry existing for 200 keV proton impact, the $\alpha(k)$ values are much higher compared to that for 66 MeV bare C ions (see Fig. 3(e)). It is to be noted that although the perturbation strength (q_p/v_p) was nearly the same for both the projectiles, yet $\alpha(k)$ showed different behaviour for both the cases, revealing that (q_p/v_p) alone cannot provide a measure for $\alpha(k)$. When the ejected electron velocity is higher than the velocity of the projectile, it is seen from Fig. 3(e) that the asymmetry parameter shows a saturation behavior however no such signature is seen for MeV energy C^{6+} ions. CDW-EIS calculations show a qualitative agreement with the experimental measurements, whereas quantitatively overestimates the data points. In addition, the present study also reveals that for low electron velocities, $\alpha(k)$ is sensitive to the structure of the target atom or molecule.

Chapter 7 : Ionization of uracil and bromouracil : keV energy protons vs MeV energy HCIs

The killing of malignant cells when irradiated by GeV energy ion beams is a promising tool for cancer treatment in recent times. When the projectile ion interacts with the biological matter, several low energy electrons (LEEs) are generated along the track which further help to create strand breakage in the DNA/RNA of the malignant cells by means of dissociative electron attachment [23]. These LEEs further react with the surrounding water molecules to create different radicals which again help in strand break of DNA/RNA. Thus the production of LEEs is the fundamental tool for killing the malignant cells. For this purpose, some of the recent studies focus on adding a high Z atom to the targeted cells, causing an amplification in electron

emission [24]. Bromouracil ($C_4H_3BrN_2O_2$) is a halouracil, where one of the H atom of uracil ($C_4H_4N_2O_2$) is replaced by a Br atom which can cause radio-biological effectiveness. Due to the high Z value of Br, several LEEs are expected to be emitted from bromouracil compared to that from uracil for the same beam energy and charge state. In this thesis work, two problems have been dealt together. Initially we have performed absolute DDCS measurements for keV energy protons and MeV energy bare C ions colliding with uracil, one of the nucleobases of RNA. In the second part, we have measured the DDCS of e^- emission from bromouracil and then present a quantitative estimate of the amount of enhancement in the electron production from bromouracil to uracil when impacted by the same projectiles.

Collision with MeV energy bare C ions

The absolute DDCS of the electrons emitted from bromouracil (BrU) in collisions with 42 and 66 MeV bare C ions were measured. The data were collected over different forward and backward emission angles. The electron energies measured varied from 1 to 600 eV whereas in a few cases measurements were performed upto 2000 eV to include the L-MM Auger line of Br. The data were compared with the prior form of the CDW-EIS calculations. These calculations were extended for the first time for such a large molecule. Overall a reasonably good agreement was observed between the calculations and the measured data. In case of 66 MeV C^{6+} ions, we have also measured the DDCS for electron emission from uracil under the same experimental conditions. These data were also compared with the CDW-EIS calculations. An effusive jet of uracil and BrU were used to perform the experiments. In addition to obtaining the DDCS and checking them with the theoretical predictions, we have derived the ratio of the DDCS of electron emission from bromouracil to that for uracil for 66 MeV bare C ions. These DDCS ratios provide a quantitative estimate for understanding the enhancement in low energy electron production from BrU compared to uracil due to the presence of a high Z atom Br. An overall enhancement of approximately 1.5 times was obtained for the different emission angles. This ratio is large compared to that estimated based on the number of electrons available and also compared to the prediction of the CDW-EIS model.

Collision with keV energy protons

To provide a comparative study on how the LEEs production varies for projectiles with different energy and charge state, we have performed DDCS measurements for ionization of BrU and uracil induced by 200 keV protons. Low Z highly charged ions like carbon and proton are the most commonly used beams for hadron therapy. Thus we have chosen both these projectiles at two different energy regimes to understand the radio-sensitizing capability of bromouracil. For absolute normalization of the DDCS, ionization cross section measurements were performed for CH_4 under similar experimental conditions. These absolute DDCS were further compared with CDW-EIS calculations. From the measurements, the SDCS and TCS were also derived by numerical integration of the DDCS. The DDCS ratios of BrU-to-uracil were also obtained. It may be seen that in both the energy range, the enhancement in electron emission are nearly the same. The large enhancement can perhaps be understood in terms of the Auger cascade decay for the Br atom. In addition, the atomic giant resonance could also contribute partially which is not well studied for Br. Finally, such enhancement is an important input for understanding the nano-sensitization

effect in case of hadron therapy.

Chapter 8 : Summary

Table 1: The collision systems studied in the present work : e^- collisions and heavy ion collisions

Target	Projectile	Energy	Source
N ₂	e^-	3 - 8 keV	Electron gun
O ₂	e^-	7 keV	Electron gun
He	H ⁺	150 & 200 keV	ECRIA
O ₂	H ⁺	200 keV	ECRIA
CH ₄	H ⁺	200 keV	ECRIA
Uracil	H ⁺	200 keV	ECRIA
Bromouracil	H ⁺	200 keV	ECRIA
O ₂	C ⁶⁺	66 MeV	Pelletron
Uracil	C ⁶⁺	66 MeV	Pelletron
Bromouracil	C ⁶⁺	42 & 66 MeV	Pelletron

In the present thesis work, we have studied the collision dynamics of different target species varying from atoms, small molecules to large biomolecules induced by fast electrons, protons and highly charged ions as shown in Table 1.

i) Detailed experimental measurements were performed to check for the existence of the Young type interference oscillations in diatomic molecules N₂ and O₂. Although for H₂, interference oscillations are known to exist, but for multielectronic targets like N₂ and O₂, earlier work suggests that oscillations are observed for photon impact, but for heavy ion impact oscillatory structures were not observed. The present studies were undertaken using fast electrons, which causes very less perturbation to the target system. Clear oscillatory structures were revealed from the DDCS ratios as well as from the forward-backward angular asymmetry for both the targets N₂ and O₂. Higher order interference oscillation was also observed for N₂.

ii) The absolute DDCS measurements for electron emission from N₂ when impacted by keV energy electrons were studied for different beam energies. All the measured data were compared with *ab initio* calculations like the CB1 model and the CTMC model calculations. The energy and angular distributions of the DDCS revealing the various features of collision mechanism like soft collision, binary nature of collision, characteristic lines originating due to inner shell ionization were extensively studied for all the collision partners. The variation of total ionization cross section with beam energy was further compared with the CSP-ic model.

iii) In order to understand how the collision dynamics changes by varying charge state and velocity, the measurements on the angular asymmetry were performed for 66 MeV C⁶⁺ ion impact on O₂ and 200 keV proton impact on He, CH₄ and O₂. All the measured DDCS were compared with the prior form of CDW-EIS calculations. The two projectiles had widely different q_p and v_p , but their perturbation strength (q_p/v_p) were nearly similar. The angular distribution showed completely different

trend for the two projectiles. Strong effect of post collisional interaction were observed in case of keV energy protons. Further, asymmetry parameter ($\alpha(k)$) not only depends on (q_p/v_p) , but changes with individual change in q_p and v_p , showing a saturation effect when the emitted electron velocity is larger than the velocity of the projectile.

iv) The DDCS measurements for ionization of uracil and bromouracil under the impact of keV energy protons and MeV energy bare C ions are reported. These measurements were compared with the CDW-EIS calculations. The DDCS ratios showed an enhancement in electron production from BrU which is much stronger than the prediction of the CDW-EIS model. Such measurements can be useful for remodeling and perhaps reducing the doses in hardon therapy. The estimation of enhancement in production of low energy electrons from the electron DDCS spectra presented in this thesis is the first of it's kind and no such direct quantitative estimate exists in the literature except another very recent study in our group for the iodouracil molecule.

References

- [1] N. Stolterfoht, R. D DuBois, and R. D Rivarola. Electron Emission in Heavy Ion-Atom Collisions. *Springer-Verlag, Berlin*, 1997.
- [2] H. D. Cohen and U. Fano. *Phys. Rev.*, 150:30, 1966.
- [3] Deepankar Misra, U. Kadhane, Y. P. Singh, L. C. Tribedi, P. D. Fainstein, and P. Richard. *Phys. Rev. Lett.*, 92:153201, 2004.
- [4] D. Misra, A. Kelkar, U. Kadhane, A. Kumar, L. C. Tribedi, and P. D. Fainstein. *Phys. Rev. A*, 74:060701, 2006.
- [5] N. Stolterfoht, B. Sulik, V. Hoffmann, B. Skogvall, J. Y. Chesnel, J. Rangama, F. Frémont, D. Hennecart, A. Cassimi, X. Husson, A. L. Landers, J. A. Tanis, M. E. Galassi, and R. D. Rivarola. *Phys. Rev. Lett.*, 87:023201, 2001.
- [6] N. Stolterfoht, B. Sulik, B. Skogvall, J. Y. Chesnel, F. Frémont, D. Hennecart, A. Cassimi, L. Adoui, S. Hossain, and J. A. Tanis. *Phys. Rev. A*, 69:012701, 2004.
- [7] M. Ilchen, L. Glaser, F. Scholz, P. Walter, S. Deinert, A. Rothkirch, J. Seltmann, J. Viefhaus, P. Decleva, B. Langer, A. Knie, A. Ehresmann, O. M. Al-Dossary, M. Braune, G. Hartmann, A. Meissner, L. C. Tribedi, M. AlKhaldi, and U. Becker. *Phys. Rev. Lett.*, 112:023001, 2014.
- [8] Saikat Nandi, Aditya N. Agnihotri, S. Kasthurirangan, Ajay Kumar, Carmen A. Tachino, Roberto D. Rivarola, F. Martín, and Lokesh C. Tribedi. *Phys. Rev. A*, 85:062705, 2012.
- [9] J. L. Baran, S. Das, F. Járαι-Szabó, K. Póra, L. Nagy, and J. A. Tanis. *Phys. Rev. A*, 78:012710, 2008.
- [10] A. N. Agnihotri, S. Kasthurirangan, S. Nandi, A. Kumar, M. E. Galassi, R. D. Rivarola, O. Fojón, C. Champion, J. Hanssen, H. Lekadir, P. F. Weck, and L. C. Tribedi. *Phys. Rev. A*, 85:032711, 2012.

- [11] S. Bhattacharjee, C. Bagdia, M. Roy Chowdhury, A. Mandal, J. M. Monti, R. D. Rivarola, and L. C. Tribedi. *Phys. Rev. A*, 100:012703, 2019.
- [12] D. Schardt, T. Elsässer, and D. Schulz-Ertner. *Rev. Mod. Phys.*, 82:383–425, 2010.
- [13] E. M. Purcell. *Phys. Rev.*, 54:818, 1938.
- [14] D. Misra, K.V. Thulasiram, W. Fernandes, A. H. Kelkar, U. Kadhane, A. Kumar, Y. Singh, L. Gulyas, and L. C. Tribedi. *Nuclear Instruments and Methods in Physics Research Section B: Beam Interactions with Materials and Atoms*, 267(1):157, 2009.
- [15] C. Champion, J. Hanssen, and P.A. Hervieux. *The Journal of Chemical Physics*, 121:9423–9429, 2004.
- [16] R. E. Olson and A. Salop. *Phys. Rev. A*, 16:531–541, 1977.
- [17] D S F Crothers and J F McCann. *Journal of Physics B: Atomic and Molecular Physics*, 16:3229–3242, 1983.
- [18] K.N. Joshipura, S. S. Gangopadhyay, H. N. Kothari, and F. A. Shelat. *Physics Letters A*, 373:2876 – 2881, 2009.
- [19] A. Messiah. Quantum Mechanics. *North-Holland, Amsterdam*, II, 1970.
- [20] P. D. Fainstein, L. Gulyás, F. Martín, and A. Salin. *Phys. Rev. A*, 53:3243, 1996.
- [21] D. Misra, A. H. Kelkar, S. Chatterjee, and L C. Tribedi. *Phys. Rev. A*, 80:062701, 2009.
- [22] S. T. Manson, L. H. Toburen, D. H. Madison, and N. Stolterfoht. *Phys. Rev. A*, 12:60–79, 1975.
- [23] B. Boudaiffa, P. Cloutier, D. Hunting, M. A. Huels, and L. Sanche. *Science*, 287:1658, 2000.
- [24] A. V. Verkhovtsev, A. V. Korol, and A. V. Solov'yov. *Phys. Rev. Lett.*, 114:063401, 2015.

List of publications

Related to thesis:

1. *Ionization of atoms and molecules using 200-keV protons and 5.5-MeV/u bare C ions : Energy-dependent collision dynamics*, **Madhusree Roy Chowdhury**, A. Mandal, A. Bhogale, H. Bansal, C. Bagdia, S. Bhattacharjee, J. M. Monti, R. D. Rivarola and Lokesh C Tribedi, **Phys. Rev. A** **102**, 012819 (2020).
2. *Double differential distributions of e-emission in ionization of N₂ by 3, 4 and 5 keV electron impact*, **Madhusree Roy Chowdhury**, Dhaval Chauhan, Chetan G. Limbachiya, Karoly Tókési, Christophe Champion, P. F. Weck and Lokesh C. Tribedi, (*accepted in J. Phys. B: At. Mol. Opt. Phys.*) (2020).
3. *Coherent electron emission from O₂ in collisions with fast electrons*, **Madhusree Roy Chowdhury**, Carlos R. Stia, Carmen A. Tachino, Omar A. Fojón, Roberto D. Rivarola and Lokesh C. Tribedi, **Eur. Phys. J. D** **71**, 218 (2017).
4. *Electron impact ionization of O₂ and the interference effect from forward–backward asymmetry*, **Madhusree Roy Chowdhury** and Lokesh C. Tribedi, **J. Phys. B: At. Mol. Opt. Phys.** **50**, 155201 (2017).
5. *Ionization of N₂ in collisions with fast electrons: Evidence of an interference effect*, **Madhusree Roy Chowdhury**, C. R. Stia, C. A. Tachino, O. A. Fojon, Roberto D. Rivarola and Lokesh C. Tribedi, **Phys. Rev. A** **94**, 052703 (2016).
6. *Differential electron emission from biomolecules under fast ion impact : Enhancement in electron emission*, **Madhusree Roy Chowdhury et. al.** (*to be submitted*)
7. *Ionization of bromouracil by keV energy protons*, **Madhusree Roy Chowdhury et. al.** (*under preparation*)

Not related to thesis:

1. *Electron emission from CH₄ molecule in collisions with fast bare C ions*, Anuvab Mandal, Chandan Bagdia, **Madhusree Roy Chowdhury**, Shamik Bhattacharjee, Deepankar Misra, Juan M. Monti, Roberto D. Rivarola and Lokesh C. Tribedi, **Phys. Rev. A** **101**, 062708 (2020).
2. *Electron emission in ionization of adenine molecule induced by 5 MeV/u bare C ions*, Shamik Bhattacharjee, Anuvab Mandal, **Madhusree Roy Chowdhury**, Chandan Bagdia, Juan M. Monti, Roberto D. Rivarola and Lokesh C Tribedi **Eur. Phys. J. D** **74**, 163 (2020).
3. *Proton capture resonant state of ¹⁵O at 7556 keV*, Sathi Sharma, Arkabrata Gupta, **M. Roy Chowdhury**, A. Mandal, A. Bisoi, V. Nanal, L. C. Tribedi, and M. Saha Sarkar, **Phys. Rev. C** **102**, 024308 (2020)

4. *Study of $^{14}\text{N}(p,\gamma)^{15}\text{O}$ resonance reaction at $E_p^{\text{lab}} = 278 \text{ keV}$* , Sathi Sharma, A. Gupta, S. Das, **M. Roy Chowdhury**, A. Mandal, A. Bisoi, V. Nanal, L.C. Tribedi, S. Sarkar and M. Saha Sarkar, **EPJ Web of Conferences** **227**, 02011 (2020).
5. *Characterization of an electrically cooled BEGe detector till $E_\gamma \sim 7 \text{ MeV}$* , Sathi Sharma, Arkabrata Gupta, Balaram Dey, **M. Roy Chowdhury**, A. Mandal, A. Bisoi, V. Nanal, L. C. Tribedi, M. Saha Sarkar **Nucl. Instr. Meth. Phys. Res. A** **964**, 163810 (2020)
6. *1s-1s electron transfer in collisions of fast C and O ions with adenine*, Chandan Bagdia, S. Bhattacharjee, **M. Roy Chowdhury**, A. Mandal, G. Lapicki and Lokesh C. Tribedi **Nucl. Instr. Meth. Phys. Res. B** **462**, 68 (2020)
7. *K-K electron capture from adenine and CO_2 molecule by fast carbon ions using KLL-Auger electron technique*, Chandan Bagdia, Shamik Bhattacharjee, **Madhusree Roy Chowdhury**, Anuvab Mandal, Gregory Lapicki, Lokesh C. Tribedi **X-Ray Spectrometry** **49**, 160 (2020).
8. *Bare-carbon-ion-impact electron emission from adenine molecules: Differential and total cross-section measurements*, Shamik Bhattacharjee, Chandan Bagdia, **Madhusree Roy Chowdhury**, J M Monti, Roberto D Rivarola and Lokesh C. Tribedi **Phys. Rev. A** **100**, 012703 (2019)
9. *M X-ray production cross-sections in ^{79}Au and ^{83}Bi induced by 50–300 keV protons* Anuvab Mandal, Shehla, **Madhusree Roy Chowdhury**, Ajay Kumar, Sanjiv Puri and Lokesh C. Tribedi **Eur. Phys. J. D** **72**, 120 (2018)
10. *Low-energy proton induced M X-ray production cross sections for ^{70}Yb , ^{81}Tl and ^{82}Pb* , Shehla, A. Mandal, Ajay Kumar, **M. Roy Chowdhury**, Sanjiv Puri and L.C. Tribedi **Nucl. Instr. Meth. Phys. Res. B** **426**, 34 (2018)
11. *Energy and angular distribution of electrons ejected from water by the impact of fast O^{8+} ion beams*, Shamik Bhattacharjee, Chandan Bagdia, **Madhusree Roy Chowdhury**, J.M. Monti, R.D. Rivarola and L.C. Tribedi **Eur. Phys. J. D** **72**, 15 (2018)
12. *Double differential distribution of electron emission in the ionization of water molecules by fast bare oxygen ions*, Shamik Bhattacharjee, Shubhadeep Biswas, Chandan Bagdia, **Madhusree Roy Chowdhury**, Saikat Nandi, Deepankar Misra, J M Monti, C A Tachino, R D Rivarola, C Champion and Lokesh C Tribedi **J. Phys. B: At. Mol. Opt. Phys.** **49**, 065202 (2016)

Conferences attended

1. *17th SPARC (Stored Particles Atomic Research Collaboration, @FAIR, GSI, Darmstadt) International Workshop*, September 14-16, 2020 (Poster presentation).
2. *26th International Symposium on Ion-Atom Collisions*, France, July 23-30, 2019 (Poster presentation).
3. *XXXIst International Conference on Photonic, Electronic and Atomic Collisions*, France, July 18-21, 2019 (Poster presentation).
4. *International Workshop on Atomic and Molecular Collisions*, India, December 10-12, 2018 (Oral presentation).
5. *13th Asian International Seminar on Atomic and Molecular Physics*, India, December 3-8, 2018 (Presented two posters).
6. *International Conference on Systems and Processes in Physics, Chemistry and Biology*, India, March 1-3, 2018 (Oral presentation).
7. *18th International Conference on Physics of Highly Charged Ions*, Poland, September 11-16, 2016 (Poster presentation).
8. *SPARC (Stored Particle Atomic Physics Research Collaboration) International Workshop*, Poland, September 16-20, 2016 (Poster presentation, **received Best poster award**).
9. *4th International Conference on Current Developments in Atomic, Molecular, Optical and Nano Physics*, India, March 11-14, 2015 (Poster presentation).